Control of UV damage repair during S phase via Dyrk1A-dependent regulation of cyclin D1/p21^{waf1cip1} stability

François Bélanger[1], Cassandra Roussel[1], Christina Sawchyn[1,2], Sari Gezzar-Dandashi[1,2], Frédérick Antoine Mallette[1,2,3], Hugo Wurtele[1,2,3,*] and Elliot Drobetsky[1,2,3, *]

1. Centre de recherche de l'Hôpital Maisonneuve-Rosemont, 5415 boulevard de l'Assomption, Montréal, H1T 2M4, Canada

2. Molecular Biology Program, Université de Montréal, 2900 Édouard-Montpetit, Montréal, Québec, Canada, H3T 1J4

3. Department of Medicine, Université de Montréal, 2900 Édouard-Montpetit, Montréal, Québec, Canada, H3T 1J4

* Co-corresponding authors

Elliot Drobetsky
elliot.drobetsky@umontreal.ca

Hugo Wurtele
hugo.wurtele@umontreal.ca

Competing interests: The authors declare no competing financial interests in relation to the work described.

ABSTRACT

Nucleotide Excision Repair (NER) eliminates highly-genotoxic solar UV-induced DNA photoproducts that otherwise stimulate malignant melanoma development. Here, a genome-wide CRISPR/Cas9 screen was exploited to uncover novel genes required for efficient NER in human cells. The screen identified Dyrk1A, a dual specificity kinase that phosphorylates the cell cycle regulator and proto-oncoprotein cyclin D1 on threonine 286 (T286), which in turn promotes its timely cytoplasmic relocalization and proteasomal degradation. Failure to modify cyclin D1 on T286 leads to nuclear accumulation of the protein, premature S phase entry, and enhanced cellular proliferation that drives tumourigenesis. We now demonstrate that Dyrk1A knockdown in UV-exposed cells causes significant inhibition of NER uniquely in S phase and reduced cell survival; moreover, both of these aberrant phenotypes were rescued upon concomitant depletion of cyclin D1. Additionally, we show (i) that expression of nonphosphorylatable cyclin D1 (T286A) interferes with NER specifically during S in a CDK-independent manner, and (ii) that this repair defect depends upon co-stabilization/upregulation of the CDK inhibitor $p21^{waf1cip1}$. Our data indicate that inhibition of NER during S phase might represent a heretofore unappreciated mechanism by which oncogenic nuclear cyclin D1 fosters melanomagenesis.

INTRODUCTION

Nucleotide excision repair (NER) is the preeminent pathway in humans for removing a wide variety of helix-destabilizing, replication and transcription-blocking DNA adducts generated by multiple environmental mutagens/carcinogens. Among such adducts are solar UV-induced cyclobutane pyrimidine dimers (CPD) and 6-4 pyrimidine-pyrimidone photoproducts (6-4PP), which represent the overriding cause of mutations promoting cutaneous tumour development[1,2]. NER comprises two overlapping sub-pathways, differing only in the mechanism of DNA damage recognition. During Global Genomic NER (GG-NER), DNA lesions are recognized throughout the genome by heterotrimeric XPC/HR23B/Centrin2 in collaboration with the E3 ligase complex UV-DDB2/UV-DDB1/Cullin4A. The other subpathway, Transcription-Coupled NER (TC-NER), acting only along the transcribed strand of active genes, is initiated when elongating RNA polymerase II stalls at damaged bases, which in turn promotes recruitment of CSB and the CSA/UV-DDB1/Cullin4A E3 ligase complex. After lesion recognition associated with either subpathway, proteins of the "core NER pathway" are sequentially recruited and function as follows: (i) The helicase and ATPase activities of XPD and XPB, respectively, as core subunits of the TFIIH basal transcription factor, mediate DNA unwinding at the damaged site; (ii) XPA partners with heterotrimeric replication protein A (RPA) to stabilize the unwound DNA and promote lesion verification in collaboration with TFIIH; (iii) The ERCC1-XPF and XPG endonucleases incise the DNA backbone on either side (5' and 3' respectively) of the lesion, producing a single-stranded DNA fragment containing the adduct which is subsequently excised; (iv) the resulting 30bp gap is resynthesized by DNA replication factors including RPA, RF-C, PCNA, and various DNA polymerases, using the damage-free complementary strand as template

and, finally, (v) DNA ligases seal the remaining nick to restore the original DNA sequence. (For review of the NER pathway see[3,4]).

The syndrome *Xeroderma pigmentosum* (XP), characterized by homozygous germline mutations in NER pathway genes and remarkable susceptibility to sunlight-induced skin cancers including malignant melanoma (MM), underscores the importance of NER to human health[5]. Thus, it may be surprising that multiple genome-wide sequencing studies have revealed a relative paucity of NER gene defects in sporadic MM within the general population[2,6,7]. On the other hand, such studies have identified numerous potential MM driver mutations, although in many cases it remains unclear how these mutations promote tumour development, and whether some might do so by negatively impacting NER efficiency.

We previously demonstrated that defective responses to DNA replication stress, e.g. in cells depleted for ATR kinase or translesion DNA polymerase eta (pol eta), can generate GG-NER defects uniquely during S phase (GG-NER during S is hereafter denoted S Phase Repair; SPR)[8–11]. As mentioned above, the RPA complex, which is essential for DNA replication, also plays a critical role in NER[12]. Excessive sequestration of RPA on ssDNA at persistently stalled replication forks (RF) or aberrantly activated origins of replication during periods of severe replication stress was shown by our group and others to limit the availability of this factor to act during NER[10,11,13]. This raises the possibility that a multitude of genes outside of the NER pathway might modulate the efficiency of UV damage repair specifically in S phase. Moreover, such genes may have thus far escaped detection because classical NER assays e.g., quantification of unscheduled DNA synthesis (UDS)[14], do not discriminate between cell cycle phases and, for technical reasons, cannot be used to evaluate repair during S.

We performed a FACS-based CRISPR/CAS9 screen in primary lung fibroblasts to identify novel genes required for efficient removal of UV-induced 6-4PP. Interestingly, this approach identified several previously unknown NER regulators that promote SPR, but do not significantly impact repair in either G1 or G2/M. Among these regulators is the dual specificity kinase Dyrk1A, which phosphorylates cyclin D1 on threonine 286 (T286)[15], thus fostering timely cytoplasmic relocalization and proteasomal degradation of the latter to regulate the G1-S transition. Interference with T286 phosphorylation leads to nuclear cyclin D1 accumulation and enhanced cellular proliferation with oncogenic consequences[16]. We demonstrate here that Dyrk1A promotes SPR efficiency and cell survival post-UV in a cyclin D1-and $p21^{waf1cip1}$-dependent manner. This indicates a novel, non-canonical mechanism whereby oncogenic cyclin D1 inhibits NER in a cell cycle-specific manner, which may harbour important implications for MM development.

RESULTS

A FACS-based CRISPR/Cas9 screen identifies novel genes regulating NER.

We previously developed an assay to quantify UV-induced 6-4PP removal as a function of cell cycle[9]. Briefly, UV- and mock-irradiated cells are co-labeled with anti-6-4PP antibody and DAPI to simultaneously monitor lesion removal and DNA content, respectively, by flow cytometry. Based on this assay, we devised a CRISPR/Cas9 loss of function screen to identify genes promoting efficient NER (Figure 1A). LF-1 primary lung fibroblasts[17] were transduced at low multiplicity of infection with pool A of the GeCKO v2 single-vector system[18], followed by 10 days of puromycin selection to remove uninfected cells. 10^8 selected cells were then irradiated with 20 J/m^2 of 254-nm UV (hereafter UV), and ones presenting high residual 6-4PP at 5h post-

irradiation were sorted by flow cytometry. Although the harsh conditions of our labeling protocol adversely affected the yield of intact single cells, we successfully sorted $1.2x10^7$ individual cells resulting in a coverage of approximately 200 genome equivalents (200X). A sample of 30 million unsorted cells was used as control to assess the sgRNA content of the transduced cell population.

sgRNA sequences were amplified from control and NER-deficient populations and sequenced. The data were analysed using MAGeCK software[19] to identify sgRNAs significantly enriched among NER-defective cells (Figure 1B and Supplementary Table 1). The top 6 hits were directly involved in the NER pathway, i.e., genes encoding XPA, XPC, and four TFIIH core subunits (GTF2H2-5), whose inactivation is fully expected to cause defects in 6-4PP removal. Moreover, other NER genes, including *XP-B, -D, -G* and *GTF2H1* exhibited significant p values (<0.05). We also found that sgRNAs targeting *POLH,* encoding pol eta, were significantly enriched in the NER-defective fraction, consistent with our previous work showing that robust pol eta expression is required for efficient SPR[8]. These data indicate that our screening strategy can be used to identify *bona fide* NER modulating genes, including ones that do so in a cell cycle-specific manner.

Gene Ontology (GO-term) analyses were performed on the top-ranking 150 genes, using an FDR cut-off of < 0.01. As expected, terms associated with NER, DNA repair, and the DNA damage response displayed significant enrichment (Supplementary Table 2). Moreover, most of the significant non-NER/-DNA repair GO-terms, e.g., chromosome organization and mRNA metabolism, were populated with NER genes, e.g., ones encoding XPA and TFIIH subunits. The number of genes populating significantly enriched GO-terms was modest (41/150), suggesting

that a variety of pathways, each represented by too few genes to reach significance in GO-term analyses, may directly or indirectly influence NER in human cells.

Among the top 50 genes we selected seven candidates, encoding proteins with no apparent involvement in NER, for validation in Hela cells: (i) *SPATC1L* (Spermatogenesis and Centriole-Associated Protein 1 Like), a germ-cell specific factor implicated in spermiogenesis[20], (ii) *CDA* (cytidine deaminase), involved in the pyrimidine salvage pathway[21] (iii) *DYRK1A* (Dual-specificity tyrosine phosphorylation-regulated kinase 1A)[22] (iv) *ZC3HC1* (a.k.a. NIPA; Nuclear Interaction Partner Of ALK), a component of an SCF-type E3 ubiquitin ligase complex regulating the G2-M transition[23] (iv) *EHD4* (EH Domain Containing 4), involved in endosomal transport[24] and (v) *C6orf62* and *ZNF182*, with no established functions. Interestingly, siRNA-mediated depletion of each of the above factors, unlike the situation for NER pathway proteins such as XPA, engendered significant defects in 6-4PP removal during S, but not during G1 or G2 (Figure 1C, Supplementary Table 3). The above results support the notion that the human genome encodes previously unknown NER regulators that promote UV DNA photoproduct removal in an S phase-specific manner.

Dyrk1A influences SPR and cellular resistance to UV by regulating cyclin D1 levels.

We chose to further characterize Dyrk1A, a dual specificity kinase that autophosphorylates on a tyrosine residue, but whose numerous substrates are modified on serines and/or threonines. This kinase exhibits broad functionality, being involved in multiple processes associated with neuronal development, transcriptional control, and cell proliferation[25]. We now demonstrate a new role for Dyrk1A, i.e., in UV damage repair; indeed siRNA-mediated knockdown of this kinase in Hela cells, in addition to causing defective SPR (Figure 1C), also promoted increased UV sensitivity as evaluated by clonogenic survival (Figure 2A).

Among the known substrates of Dyrk1A is cyclin D1, a cell cycle regulator that complexes with CDK4/6 to control the G1-S transition[26]. Dyrk1A phosphorylates cyclin D1 on T286, which targets the latter for timely nuclear export and proteolytic degradation, thus preventing premature entry into S phase[15]. As expected, RNAi knockdown of Dyrk1A in Hela cells (i) increased cyclin D1 abundance and the proportion of cells in S phase (Figure 2B) and, (ii) significantly reduced the rate of DNA synthesis, as assessed by EdU incorporation (Figure 2C); moreover, concomitant knockdown of cyclin D1 reversed each of these phenotypes (Figure 2B-C). Strikingly, depletion of cyclin D1 also rescued both the SPR defect and UV sensitivity caused by lack of Dyrk1A (Figure 2D-E). However, knockdown of cyclin D1 did not rescue defective SPR caused by ATR inhibition[9] (Figure 2F) indicating that lack of cyclin D1 does not promote NER during S non-specifically in cells expressing Dyrk1A. These data show that Dyrk1A-dependent regulation of cyclin D1 levels is required for efficient repair of UV-induced DNA photoproducts uniquely during S phase in human cells.

Defective SPR upon Dyrk1A depletion is not attributable to abnormal cell cycle progression or reduced RPA availability.

As mentioned earlier, mutations causing increased replicative stress can engender SPR defects due to excessive sequestration of RPA on ssDNA at stalled RF and/or aberrantly activated origins of replication[10,11,13]. Moreover, reduced G1 duration compromises loading of the MCM helicase complex onto origin DNA[27], which diminishes the number of active RF and causes replicative stress[28]. Since Dyrk1A knock-down was shown to shorten G1[15], we tested whether this circumstance might generate replicative stress and consequent SPR defects. We found that in S phase cells, Dyrk1A depletion diminished chromatin-bound levels of the MCM helicase subunit MCM7 and of the DNA replication processivity clamp PCNA (Figure 3A-B), consistent

with a reduced number of active RF. To probe whether this might compromise SPR, we treated Hela cells with PHA-767491, a pharmacological inhibitor of Cdc7 kinase whose activity is essential for activation of DNA replication origins[29]. Similar to the effect of Dyrk1A depletion, Cdc7i treatment caused accumulation of cells in S, reduced EdU incorporation, and diminished levels of chromatin-bound PCNA (Figure 3C-D). However, Cdc7i did not inhibit 6-4PP excision during S (Figure 3E). Depletion of the Anaphase-Promoting Complex (APC) regulator FZR1 is also known to shorten G1[30]. While progression through G1 and S was similar in Dyrk1A- and FZR1-depleted cells (Supplementary Figure 1A, Supplementary Table 3), the latter remained SPR-proficient (Supplementary Figure 1B). We conclude that defective SPR caused by Dyrk1A depletion and concomitant cyclin D1 stabilization is not due to shortened G1 or reduced numbers of active RF.

We then directly examined the impact of Dyrk1A on the UV-induced replicative stress response. Phosphorylation of histone H2AX(S139), Chk1(S345) and RPA32(S33), well-known markers for activation of replicative stress-induced signalling, were not elevated post-UV in Dyrk1A-depleted vs control Hela cells (Figure 3F-G). We also found that levels of DNA-bound RPA were significantly reduced upon Dyrk1A depletion in response to either HU or UV versus non-targeting siRNA controls (Figure 3H). This likely reflects reduction in the number of active DNA RF (Figure 3A-B) since depletion of Dyrk1A did not decrease either the total amount (Figure 3I, left panel) or nuclear localization/abundance of RPA subunits (Figure 3I, right panel). SPR defects upon Dyrk1A depletion are therefore unlikely to be caused by decreased RPA availability due to elevated recruitment of this complex to stalled RF.

Nuclear cyclin D1 overexpression is associated with SPR defects in melanoma cell lines.

We previously reported that a majority of human melanoma cell lines are characterized by defective SPR, although the molecular mechanism remains unclear[31]. Since cyclin D1 is overexpressed with oncogenic consequences in various cancers including melanoma[16], we examined its levels in three SPR-proficient and four SPR-deficient MM cell lines. While cyclin D1 expression did not strictly correlate with SPR status, SPR-deficient WM278 and 451Lu exhibited the highest expression of this protein (Figure 4A). Remarkably, siRNA-mediated depletion of cyclin D1 rescued defective SPR in both of these lines (Figure 4B).

We then expressed WT cyclin D1 and the non-phosphorylatable variant cyclin D1(T286A), both epitope-tagged with Flag-HA, in the SPR-proficient melanoma cell line WM1366 which exhibits relatively low expression of endogenous cyclin D1 (Figure 4A). As expected[15], levels of nonphosphorylatable cyclin D1(T286A)-Flag-HA were much higher than the WT counterpart (Figure 4C). The overexpressed T286A variant was functional since it elevated Rb phosphorylation and the fraction of cells in S, both of which were reversed by pharmacological inhibition of CDK4/6 using palbociclib (Figure 4D-E). Importantly, overexpression of cyclin D1 (T286A) caused SPR defects in WM1366 MM cells (Figure 4F) and LF-1 primary lung fibroblasts (Supplementary Figure 2). Pre-treatment with palbociclib did not rescue the SPR defect caused by cyclin D1(T286A) expression (Figure 4F), indicating that appropriate regulation of cyclin D1 stability is required for robust UV damage repair during S in a CDK-independent manner.

Consistent with its negative impact on SPR, we observed that in WM1366 cells cyclin D1(T286A) expression increased UV-induced cytotoxicity (Figure 4G). This was accompanied by elevated DNA double-strand break (DSB) formation at 16 h post-UV, as assessed by induction of histone H2AX(S139) and 53BP1(S1778) phosphorylation (Figure 4H). It appears

unlikely that such DSB are due to apoptosis-associated nucleolytic DNA fragmentation[32,33], since (i) well established markers of apoptosis, i.e., caspase 3- and PARP1-cleavage, were not detected at 16 h post-UV in WM1366 (Figure 4I) and (ii) this cell line appears relatively resistant to apoptosis, as staurosporine treatment did not cause either PARP1- or Caspase 3-cleavage, in contrast to the situation for Hela cells (Figure 4I). These data indicate that nuclear overexpresion of cyclin D1, leading to inhibition of NER specifically during S, eventually causes lethal DSB and cell death in melanoma cells post-UV.

Defective SPR caused by interference with Dyrk1A-mediated phosphorylation of cyclin D1 depends upon co-stabilization of p21^{waf1cip1}.

Dyrk1A-depletion was previously shown to enhance p21^{waf1cip1} (hereafter p21) expression in a cyclin D1-dependent manner[15]. Consistently, we observed an increase in p21 abundance upon expression of cyclin D1(T286A) in WM1366 cells (Figure 5A). Elevated levels of these proteins were observed in the nuclei of both S phase (EdU+) and G1/G2 (EdU-) cells (Figure 5B-C). Depletion of p21 further increased the proportion of S phase cells expressing cyclin D1(T286A) as previously reported[15] and, remarkably, resulted in rescue of their SPR defect (Figure 5D). Since p21 was shown to inhibit DNA replication by binding PCNA[34,35], multiple studies have focused on the possibility that the former protein might also harbour the capacity to abrogate NER gap filling by sequestering PCNA; however any role for p21 in UV damage repair remains controversial (see Discussion). Interestingly, previous studies showed that UV DNA photoproduct excision is coupled to post-incision NER gapfilling[36,37], such that defects in gapfilling also inhibit photoproduct removal[38]. However, unlike the expected situation for cells knocked down for XPA, we found that depletion of Dyrk1A does not cause defective UDS post-UV in G1 cells (Figure 5E). Overall, these results indicate that elevation in p21 expression is the

root cause of cyclin D1 (T286A)-dependent defects in UV photoproduct removal specifically during S phase.

DISCUSSION

We performed a FACS-based CRISPR/Cas9 screen to identify genes implicated in the removal of UV-induced 6-4PP via NER. To our knowledge, this represents the first genome-wide functional screen where the efficiency of UV damage repair *per se* is the experimental endpoint. While genes encoding known NER factors were well-represented among the top hits, we also recovered pol eta, which is known to mediate replicative bypass of UV-induced CPD[39]; moreover as mentioned above lack of this translesion DNA polymerase abrogates NER uniquely during S phase[8]. This provided confidence in our screening strategy, and showed that it can identify genes which influence UV damage repair in a cell cycle-specific manner. Remarkably, depletion of the seven genes selected for validation in the present study, which are representative of multiple cellular pathways with no previous implication in NER, engendered significant UV damage repair defects strictly in S phase (Figure 1). As discussed earlier, we and others previously demonstrated that such defects can be caused by abnormal replicative stress responses, leading to excessive sequestration of RPA *in trans* at persistently stalled RF, which in turn prevents the essential action of this complex in NER[10,11,13]. Our published results also indicate that SPR defects (i) are frequent in model MM cell lines[31] and (ii) strongly associated with chemosensitivity in ovarian cancer[11], highlighting the potential biological and clinical relevance of this phenotype. Overall, our findings suggest that a substantial proportion of NER-modulating genes within the human genome encode proteins that significantly influence UV damage repair specifically during S phase. Further investigation will be required to evaluate

whether replicative stress-associated RPA sequestration, or other mechanisms, underlie SPR defects caused by lack of such new NER regulators.

Among the aforementioned seven genes, we focused on one encoding the dual specificity kinase Dyrk1A, which regulates multiple cellular pathways implicated in neurogenesis, transcription, cell cycle control, and cancer development[40]. In view of our previous work, we initially suspected that Dyrk1A knockdown might reduce SPR efficiency via deregulation of the replicative stress response. However, our data clearly demonstrate that classical markers of UV-induced replicative stress, including ssDNA-RPA generation and phosphorylation of histone H2AX and Chk1, are not elevated upon depletion of Dyrk1A. Rather we found that Dyrk1A regulates SPR through phosphorylation of cyclin D1 on T286[15], a modification that promotes its nuclear export and proteolytic degradation[41,42]. In complex with CDK4/6, cyclin D1 promotes phosphorylation of retinoblastoma protein leading to E2F transcription factor activation and consequent expression of genes required for the G1-S transition[26]. As such Dyrk1A-dependent phosphorylation of cyclin D1 contributes to the prevention of premature entry into S phase[15]. Our combined results in Hela and melanoma cells now show that abrogation of Dyrk1A leading to nuclear accumulation of cyclin D1 significantly inhibits NER specifically during S phase in a CDK-independent manner. It should be mentioned that in addition to Dyrk1A, other cellular kinases including GSK3β, ERK1/2, and p38 have been shown to phosphorylate cyclin D1 on T286, which can also promote its cytoplasmic relocalization/proteasomal degradation[43,44]. Nonetheless, in our hands, loss of Dyrk1A alone was sufficient to significantly stabilize and upregulate nuclear cyclin D1.

Cyclin D1 is a major driver of multiple cancers[45] including MM[46], through overexpression in either the cytoplasm or nucleus, where it promotes tumour invasion/metastasis,

or deregulation of cell cycle control, respectively. To exert an oncogenic role, nuclear cyclin D1 must be aberrantly stabilized/overexpressed in conjunction with inhibition of its cytoplasmic relocalization[47], as exemplified by the situation for the nonphosphorylatable cyclin D1(T286A) variant used here[41]. A number of reports have revealed non-canonical CDK-dependent and -independent roles for nuclear cyclin D1, notably in transcription and DNA double-strand break repair[48,49]. In addition, nuclear cyclin D1 is known to associate with the essential DNA replication factor PCNA[50–52], thereby forestalling its interaction with DNA polymerases to inhibit DNA synthesis[50]. One early investigation indicated that, in UV-exposed human fibroblasts, cyclin D1 overexpression inhibits PCNA-dependent NER gapfilling during G1[53]. Our data are not consistent with this, since quantification of UDS by EdU incorporation in Hela cells revealed no significant impairment of NER gapfilling in either G1 or G2 post-UV upon Dyrk1A knockdown (Figure 5E).

Another feature of the current study that differentiates it from the aforementioned one regards our finding that Dyrk1A knockdown and concomitant cyclin D1 nuclear accumulation, while not generating significant NER defects in G1/G2, does so uniquely during S phase. Moreover, we show that depletion of p21 completely rescues defective SPR caused by cyclin D1 (T286A) expression, without reducing levels of the latter. Our overall results thus indicate that upon Dyrk1A depletion, upregulation of p21, rather than of cyclin D1 *per se*, causes SPR defects.

p21 strongly binds the essential DNA replication factor PCNA via a canonical PIP box motif[54]. However, while there is general agreement that p21 can interfere with DNA replication via PCNA interaction, any influence of p21 on PCNA-dependent gapfilling during NER, or any other step of this repair pathway, remains controversial. Two early studies using human cell-free

extracts reported that p21 exerts no effect on PCNA-dependent NER gapfilling[55,56], while another indicated that p21strongly inhibits this process[57]. Yet another investigation supported this latter result *in vitro*, as well as *in vivo*[58]. While, as discussed earlier, our data indicate that Dyrk1A depletion and consequent cyclin D1/p21 overexpression does not negatively impact NER gapfilling during G1 or G2, the possibility of such an impact in S but not other phases cannot be ruled out. However we emphasize that evaluation by UDS of NER gapfilling during S is technically unfeasible, since comparatively weak EdU incorporation signals emanating from this process are dwarfed by those resulting from chromosomal DNA replication[14]. Further investigation will be necessary to characterize the precise mechanism by which Dyrk1A-dependent destabilization of cyclin D1 and p21 promotes NER specifically during S phase.

Overwhelming epidemiological and molecular evidence demonstrate that induction of UV-induced DNA damage during sunlight exposure is a critical determinant in the initiation of cutaneous tumors. While *a priori* this portends a primary role for NER in protection against MM, to date very few data support the plausible expectation that sporadic MM is frequently characterized by NER defects. (One exception is provided by our own work cited earlier showing that a majority of human MM cell lines exhibit defective SPR[31].) We posit that this paucity of data may be attributable, in part, to the fact that previous studies probing the influence of NER on MM development have not considered the possibility that this repair pathway might be defective during S and not other phases. Herein we exploited a cell cycle-specific NER assay to show that aberrant accumulation of cyclin D1 in the nucleus, which can arise through any among multiple mechanisms[45], promotes the inhibition of NER specifically during S phase. As such, our data indicate a potential novel noncanonical role for oncogenic nuclear cyclin D1 in the development of solar UV-induced MM, as well as of other major

cancers. Indeed, carcinoma of the lung and liver, both of which frequently express oncogenic cyclin D, are strongly promoted by exposure to environmental mutagens (i.e., benzo(a)pyrene) and aflatoxin B1, respectively) that generate adducts repaired exclusively by NER.

MATERIALS AND METHODS

Cell culture

LF-1 primary human lung fibroblasts[17], a gift from Dr John Sedivy (Brown University), were grown in Eagle's MEM containing 15% FBS, essential and nonessential amino acids, vitamins and antibiotics (Life Technologies, Carlsbad, CA, USA). Hela cells (ATCC; Manassas, VA, USA) were cultured in DMEM + 10% FBS and antibiotics. Melanoma cell lines (Coriell Institute; Camden, NJ, USA) were cultured as described[31]. All cell lines were authenticated by STR analysis (McGill University Genome Center, Montreal, Canada), and routinely tested for mycoplasma contamination by DAPI stain.

Reagents and plasmids

Chemical inhibitors, antibodies, siRNAs and DNA oligonucleotides are listed in Supplementary Materials and Methods. *CCND1* WT and T286A were PCR amplified from pcDNA-cyclinD1-HA[59] (Addgene plasmids # 11181 and 11182) and cloned into pDONR221 using Gateway BP Clonase (Life Technologies). Entry clones were recombined with MSCV-N-Flag-HA-IRES-PURO[60] (Addgene plasmid # 41033) using Gateway LR Clonase II (Life Technologies). Plasmids and siRNAs were transfected using Lipofectamine 2000 and RNAiMax (Life Technologies).

CRISPR screen

The human GeCKOv2 CRISPR knockout pooled library (Addgene #1000000048) was used as described[18]. 100 million sgRNA-transduced LF-1 cells were irradiated with 20 J/m^2 UV, labeled with DAPI and anti-6-4PP antibody at 5h post-irradiation, and NER-deficient cells sorted using flow cytometry[31]. Genomic DNA was isolated and quantified with PicoGreen (Life Technologies) using a TBS-380 fluorimeter (Turner Biosystems, Sunnyvale, CA, USA). PCR of genomic DNA and next generation sequencing were carried out as described[18] (see Supplementary Materials and Methods for details). Sequencing adaptors were removed using cutadapt[61]. MAGeCK software version 0.5.6[19] was used to generate sgRNA read count data, enriched guides, and gene-level rankings. GO term enrichment was performed using the preranked tool from the GSEA desktop app version 4.1.0 and the Molecular Signatures Database version 7.2[62,63]. The relative contribution of each gene was ranked by its -log10(P value), as obtained by MAGeCK analysis.

Clonogenic survival.

Clonogenic survival was evaluated as described[31].

Immunoblotting.

Immunoblotting was performed on whole cell extracts using standard protocols. Antibodies are listed in Supplementary Materials and Methods. Imaging was performed using ECL prime reagent (GE healthcare, Chicago, IL, USA) with an Azure c600 instrument (Azure Biosystems, Dublin, CA, USA).

Flow cytometry

6-4PP removal was quantified as described[31]. Cell cycle analysis and detection of chromatin-bound proteins were performed as described[64], with the following modifications in the case of PCNA and MCM7: After fixation, cells were resuspended in 0.5 mL PBSB (PBS + 0.1% BSA),

mixed with 3 mL of -20 ºC methanol and incubated at -20 ºC for 15 min. Cells were pelleted at 1500 rpm for 2 min at 4 °C, washed with 2 mL of PBSB, and washed again with 0.5 mL of 1X BD Perm/Wash buffer before antibody labeling. Data acquisition was performed on an LSR II flow cytometer (BD Biosciences, Franklin Lakes, NJ, USA) and analysed using FlowJo software v10 (Ashland, OR, USA).

Immunofluorescence microscopy.

For detection of total RPA32 and RPA70, cells were pulsed with 10 µM EdU for 20 min, washed with PBS, and fixed with 4% formaldehyde in PBS for 30 min at room temperature. Cells were permeabilized in 0.1% triton X100 in PBS for 10 min, followed by blocking in PBS containing 3% BSA overnight at 4 ºC. Primary antibodies were incubated for 3 h at room temperature. EdU was labeled with Alexa 647 followed by DAPI, as described[64]. Detection of p21 was performed as above except that 0.2% Triton X-100 was used and blocking was at room temperature in PBS + 3% goat serum + 0.05% Tween-20 for 1 h. Primary antibody was incubated overnight at 4 ºC. Images were acquired with a DeltaVision Elite system (GE Healthcare). Nuclear fluorescence signals were quantified using custom software as described[10].

Unscheduled DNA synthesis

NER gap filling was evaluated by unscheduled DNA synthesis assay as described[65]. Nuclear fluorescence signals were quantified using custom software as described[10]. Cells in S-phase with high EdU signal were excluded from the analysis.

ACKNOWLEDGEMENTS

This work was supported by the following Canadian Institutes of Health Research (CIHR)

operating grants: 201603PJT-364096 to E.A.D., 201709PJT-388346 to H.W., and MOP-133442 to F.A.M. H.W. is the recipient of a Fonds de la recherche du Québec-Santé (FRQS) Senior scholarship (award #281795). C.S. holds Ph.D scholarships from the FRQS and Cole Foundation. F.A.M. holds a Canada Research Chair in Epigenetics of Aging and Cancer.

DATA AVAILABILITY STATEMENT

The datasets generated during and/or analysed during the current study are available from the corresponding author on reasonable request.

COMPETING INTERESTS

The authors declare no competing financial interests in relation to the work described.

REFERENCES

1 Brash DE, Rudolph JA, Simon JA, Lin A, McKenna GJ, Baden HP *et al.* A role for sunlight in skin cancer: UV-induced p53 mutations in squamous cell carcinoma. *Proc Natl Acad Sci USA* 1991; **88**: 10124–10128.

2 Hodis E, Watson IR, Kryukov GV, Arold ST, Imielinski M, Theurillat J-P *et al.* A Landscape of Driver Mutations in Melanoma. *Cell* 2012; **150**: 251–263.

3 Marteijn JA, Lans H, Vermeulen W, Hoeijmakers JHJ. Understanding nucleotide excision repair and its roles in cancer and ageing. *Nat Rev Mol Cell Biol* 2014; **15**: 465–481.

4 Lans H, Hoeijmakers JHJ, Vermeulen W, Marteijn JA. The DNA damage response to transcription stress. *Nature Reviews Molecular Cell Biology* 2019; **20**: 766–784.

5 DiGiovanna JJ, Kraemer KH. Shining a light on xeroderma pigmentosum. *J Invest Dermatol* 2012; **132**: 785–796.

6 Akbani R, Akdemir KC, Aksoy BA, Albert M, Ally A, Amin SB *et al.* Genomic Classification of Cutaneous Melanoma. *Cell* 2015; **161**: 1681–1696.

7 Berger MF, Hodis E, Heffernan TP, Deribe YL, Lawrence MS, Protopopov A *et al.* Melanoma genome sequencing reveals frequent PREX2 mutations. *Nature* 2012; **485**: 502–506.

8 Auclair Y, Rouget R, Belisle JM, Costantino S, Drobetsky EA. Requirement for functional DNA polymerase eta in genome-wide repair of UV-induced DNA damage during S phase. *DNA Repair (Amst)* 2010; **9**: 754–764.

9 Auclair Y, Rouget R, Affar EB, Drobetsky EA. ATR kinase is required for global genomic nucleotide excision repair exclusively during S phase in human cells. *Proc Natl Acad Sci USA* 2008; **105**: 17896–17901.

10 Bélanger F, Angers J-P, Fortier E, Hammond-Martel I, Costantino S, Drobetsky E *et al.* Mutations in Replicative Stress Response Pathways Are Associated with S Phase-Specific Defects in Nucleotide Excision Repair. *J Biol Chem* 2015. doi:10.1074/jbc.M115.685883.

11 Bélanger F, Fortier E, Dubé M, Lemay J-F, Buisson R, Masson J-Y *et al.* Replication Protein A Availability during DNA Replication Stress Is a Major Determinant of Cisplatin Resistance in Ovarian Cancer Cells. *Cancer Res* 2018; **78**: 5561–5573.

12 He Z, Henricksen LA, Wold MS, Ingles CJ. RPA involvement in the damage-recognition and incision steps of nucleotide excision repair. *Nature* 1995; **374**: 566–569.

13 Tsaalbi-Shtylik A, Moser J, Mullenders LHF, Jansen JG, de Wind N. Persistently stalled replication forks inhibit nucleotide excision repair in trans by sequestering Replication protein A. *Nucleic Acids Res* 2014; **42**: 4406–4413.

14 Kelly CM, Latimer JJ. Unscheduled DNA Synthesis. *Methods Mol Biol* 2005; **291**: 303–320.

15 Chen J-Y, Lin J-R, Tsai F-C, Meyer T. Dosage of Dyrk1a shifts cells within a p21-cyclin D1 signaling map to control the decision to enter the cell cycle. *Mol Cell* 2013; **52**: 87–100.

16 Musgrove EA, Caldon CE, Barraclough J, Stone A, Sutherland RL. Cyclin D as a therapeutic target in cancer. *Nat Rev Cancer* 2011; **11**: 558–572.

17 Brown JP, Wei W, Sedivy JM. Bypass of senescence after disruption of p21CIP1/WAF1 gene in normal diploid human fibroblasts. *Science* 1997; **277**: 831–834.

18 Sanjana NE, Shalem O, Zhang F. Improved vectors and genome-wide libraries for CRISPR screening. *Nat Methods* 2014; **11**: 783–784.

19 Li W, Xu H, Xiao T, Cong L, Love MI, Zhang F *et al.* MAGeCK enables robust identification of essential genes from genome-scale CRISPR/Cas9 knockout screens. *Genome Biol* 2014; **15**: 554.

20 Kim J, Kwon JT, Jeong J, Kim J, Hong SH, Kim J *et al.* SPATC1L maintains the integrity of the sperm head-tail junction. *EMBO Rep* 2018; **19**: e45991.

21 Frances A, Cordelier P. The Emerging Role of Cytidine Deaminase in Human Diseases: A New Opportunity for Therapy? *Mol Ther* 2020; **28**: 357–366.

22 Laham AJ, Saber-Ayad M, El-Awady R. DYRK1A: a down syndrome-related dual protein kinase with a versatile role in tumorigenesis. *Cell Mol Life Sci* 2021; **78**: 603–619.

23 Bassermann F, von Klitzing C, Münch S, Bai R-Y, Kawaguchi H, Morris SW *et al.* NIPA defines an SCF-type mammalian E3 ligase that regulates mitotic entry. *Cell* 2005; **122**: 45–57.

24 Sharma M, Naslavsky N, Caplan S. A role for EHD4 in the regulation of early endosomal transport. *Traffic* 2008; **9**: 995–1018.

25 Fernández-Martínez P, Zahonero C, Sánchez-Gómez P. DYRK1A: the double-edged kinase as a protagonist in cell growth and tumorigenesis. *Mol Cell Oncol* 2015; **2**: e970048.

26 Sherr CJ. D-type cyclins. *Trends Biochem Sci* 1995; **20**: 187–190.

27 Matson JP, Dumitru R, Coryell P, Baxley RM, Chen W, Twaroski K *et al.* Rapid DNA replication origin licensing protects stem cell pluripotency. *Elife* 2017; **6**: e30473.

28 Ahuja AK, Jodkowska K, Teloni F, Bizard AH, Zellweger R, Herrador R *et al.* A short G1 phase imposes constitutive replication stress and fork remodelling in mouse embryonic stem cells. *Nat Commun* 2016; **7**. doi:10.1038/ncomms10660.

29 Remus D, Diffley JF. Eukaryotic DNA replication control: Lock and load, then fire. *Current Opinion in Cell Biology* 2009; **21**: 771–777.

30 Sigl R, Wandke C, Rauch V, Kirk J, Hunt T, Geley S. Loss of the mammalian APC/C activator FZR1 shortens G1 and lengthens S phase but has little effect on exit from mitosis. *J Cell Sci* 2009; **122**: 4208–4217.

31 Bélanger F, Rajotte V, Drobetsky EA. A majority of human melanoma cell lines exhibits an S phase-specific defect in excision of UV-induced DNA photoproducts. *PLoS ONE* 2014; **9**: e85294.

32 Panzarino NJ, Krais JJ, Cong K, Peng M, Mosqueda M, Nayak SU *et al.* Replication Gaps Underlie BRCA Deficiency and Therapy Response. *Cancer Res* 2021; **81**: 1388–1397.

33 Rogakou EP, Nieves-Neira W, Boon C, Pommier Y, Bonner WM. Initiation of DNA fragmentation during apoptosis induces phosphorylation of H2AX histone at serine 139. *J Biol Chem* 2000; **275**: 9390–9395.

34 Waga S, Hannon GJ, Beach D, Stillman B. The p21 inhibitor of cyclin-dependent kinases controls DNA replication by interaction with PCNA. *Nature* 1994; **369**: 574–578.

35 Flores-Rozas H, Kelman Z, Dean FB, Pan ZQ, Harper JW, Elledge SJ *et al.* Cdk-interacting protein 1 directly binds with proliferating cell nuclear antigen and inhibits DNA replication catalyzed by the DNA polymerase delta holoenzyme. *Proc Natl Acad Sci U S A* 1994; **91**: 8655–8659.

36 Mocquet V, Lainé JP, Riedl T, Yajin Z, Lee MY, Egly JM. Sequential recruitment of the repair factors during NER: the role of XPG in initiating the resynthesis step. *EMBO J* 2008; **27**: 155–167.

37 Staresincic L, Fagbemi AF, Enzlin JH, Gourdin AM, Wijgers N, Dunand-Sauthier I *et al.* Coordination of dual incision and repair synthesis in human nucleotide excision repair. *EMBO J* 2009; **28**: 1111–1120.

38 Kemp MG, Gaddameedhi S, Choi J-H, Hu J, Sancar A. DNA repair synthesis and ligation affect the processing of excised oligonucleotides generated by human nucleotide excision repair. *J Biol Chem* 2014; **289**: 26574–26583.

39 Sale JE, Lehmann AR, Woodgate R. Y-family DNA polymerases and their role in tolerance of cellular DNA damage. *Nat Rev Mol Cell Biol* 2012; **13**: 141–152.

40 Rammohan M, Harris E, Bhansali RS, Zhao E, Li LS, Crispino JD. The chromosome 21 kinase DYRK1A: emerging roles in cancer biology and potential as a therapeutic target. *Oncogene* 2022. doi:10.1038/s41388-022-02245-6.

41 Alt JR, Cleveland JL, Hannink M, Diehl JA. Phosphorylation-dependent regulation of cyclin D1 nuclear export and cyclin D1-dependent cellular transformation. *Genes Dev* 2000; **14**: 3102–3114.

42 Lin DI, Barbash O, Kumar KGS, Weber JD, Harper JW, Klein-Szanto AJP *et al.* Phosphorylation-dependent ubiquitination of cyclin D1 by the SCF(FBX4-alphaB crystallin) complex. *Mol Cell* 2006; **24**: 355–366.

43 Diehl JA, Cheng M, Roussel MF, Sherr CJ. Glycogen synthase kinase-3beta regulates cyclin D1 proteolysis and subcellular localization. *Genes Dev* 1998; **12**: 3499–3511.

44 Densham RM, Todd DE, Balmanno K, Cook SJ. ERK1/2 and p38 cooperate to delay progression through G1 by promoting cyclin D1 protein turnover. *Cell Signal* 2008; **20**: 1986–1994.

45 Tchakarska G, Sola B. The double dealing of cyclin D1. *Cell Cycle* 2020; **19**: 163–178.

46 González-Ruiz L, González-Moles MÁ, González-Ruiz I, Ruiz-Ávila I, Ayén Á, Ramos-García P. An update on the implications of cyclin D1 in melanomas. *Pigment Cell Melanoma Res* 2020; **33**: 788–805.

47 Kim JK, Diehl JA. Nuclear cyclin D1: an oncogenic driver in human cancer. *J Cell Physiol* 2009; **220**: 292–296.

48 Bienvenu F, Jirawatnotai S, Elias JE, Meyer CA, Mizeracka K, Marson A *et al.* Transcriptional role of cyclin D1 in development revealed by a genetic-proteomic screen. *Nature* 2010; **463**: 374–378.

49 Jirawatnotai S, Hu Y, Michowski W, Elias JE, Becks L, Bienvenu F *et al.* A function for cyclin D1 in DNA repair uncovered by protein interactome analyses in human cancers. *Nature* 2011; **474**: 230–234.

50 Fukami-Kobayashi J, Mitsui Y. Cyclin D1 inhibits cell proliferation through binding to PCNA and cdk2. *Exp Cell Res* 1999; **246**: 338–347.

51 Matsuoka S, Yamaguchi M, Matsukage A. D-type cyclin-binding regions of proliferating cell nuclear antigen. *J Biol Chem* 1994; **269**: 11030–11036.

52 Xiong Y, Zhang H, Beach D. D type cyclins associate with multiple protein kinases and the DNA replication and repair factor PCNA. *Cell* 1992; **71**: 505–514.

53 Pagano M, Theodoras AM, Tam SW, Draetta GF. Cyclin D1-mediated inhibition of repair and replicative DNA synthesis in human fibroblasts. *Genes Dev* 1994; **8**: 1627–1639.

54 Mansilla SF, de la Vega MB, Calzetta NL, Siri SO, Gottifredi V. CDK-Independent and PCNA-Dependent Functions of p21 in DNA Replication. *Genes (Basel)* 2020; **11**: E593.

55 Shivji MK, Grey SJ, Strausfeld UP, Wood RD, Blow JJ. Cip1 inhibits DNA replication but not PCNA-dependent nucleotide excision-repair. *Curr Biol* 1994; **4**: 1062–1068.

56 Li R, Waga S, Hannon GJ, Beach D, Stillman B. Differential effects by the p21 CDK inhibitor on PCNA-dependent DNA replication and repair. *Nature* 1994; **371**: 534–537.

57 Pan ZQ, Reardon JT, Li L, Flores-Rozas H, Legerski R, Sancar A *et al.* Inhibition of nucleotide excision repair by the cyclin-dependent kinase inhibitor p21. *J Biol Chem* 1995; **270**: 22008–22016.

58 Cooper MP, Balajee AS, Bohr VA. The C-terminal domain of p21 inhibits nucleotide excision repair In vitro and In vivo. *Mol Biol Cell* 1999; **10**: 2119–2129.

59 Newman RM, Mobascher A, Mangold U, Koike C, Diah S, Schmidt M *et al.* Antizyme targets cyclin D1 for degradation. A novel mechanism for cell growth repression. *J Biol Chem* 2004; **279**: 41504–41511.

60 Sowa ME, Bennett EJ, Gygi SP, Harper JW. Defining the human deubiquitinating enzyme interaction landscape. *Cell* 2009; **138**: 389–403.

61 Martin M. CUTADAPT removes adapter sequences from high-throughput sequencing reads. *EMBnet.journal* 2011; **17**: 10–12.

62 Subramanian A, Tamayo P, Mootha VK, Mukherjee S, Ebert BL, Gillette MA *et al.* Gene set enrichment analysis: a knowledge-based approach for interpreting genome-wide expression profiles. *Proc Natl Acad Sci U S A* 2005; **102**: 15545–15550.

63 Liberzon A, Subramanian A, Pinchback R, Thorvaldsdóttir H, Tamayo P, Mesirov JP. Molecular signatures database (MSigDB) 3.0. *Bioinformatics* 2011; **27**: 1739–1740.

64 Forment JV, Jackson SP. A flow cytometry-based method to simplify the analysis and quantification of protein association to chromatin in mammalian cells. *Nat Protoc* 2015; **10**: 1297–1307.

65 Limsirichaikul S, Niimi A, Fawcett H, Lehmann A, Yamashita S, Ogi T. A rapid non-radioactive technique for measurement of repair synthesis in primary human fibroblasts by incorporation of ethynyl deoxyuridine (EdU). *Nucleic Acids Res* 2009; **37**: e31.

FIGURE LEGENDS

Figure 1: A CRISPR/CAS9 screen identifies genes that influence NER

A) Primary human lung fibroblasts (LF-1) were infected with the GeCKO v2 lentiviral library. A FACS-based NER assay was used to sort cells characterized by reduced efficiency of 6-4PP removal at 5h post-UV. B) MAGeCK software was used to assign an RRA score and p value for each gene. Known GG-NER genes are shown in red and *POLH* in blue. The grey line delineates genes that are significantly enriched in the NER defective fraction. C) Candidate genes were

knocked down individually in Hela cells using siRNA. Left: representative bivariate plots of 6-4PP removal as a function of cell cycle for cells treated with siRNA against *POLH* or non-targeting (NT) control. Right: 6-4PP remaining 5h post-UV as a function of cell cycle for individual candidates following siRNA knockdown. XPA represents an NER deficient control. P-values compare the percentage of damage remaining in S for each siRNA vs NT control (unpaired t test: ** $p < 0.01$; ***$p < 0.001$). Values are means +/- SD of at least 3 independent experiments.

Figure 2: Dyrk1A influences NER in Hela cells by regulating cyclin D1 stability

A) Clonogenic survival post-UV +/- siRNA targeting Dyrk1A. B) Left: Immunoblot from total cell extracts treated with siRNA against Dyrk1A and/or cyclin D1. Middle and right: cell cycle distribution assessed by DNA content analysis (DAPI). C) DNA synthesis quantified by EdU incorporation +/-siRNA against Dyrk1A and/or cyclin D1. D) Quantification of 6-4PP removal +/-siRNA against Dyrk1A and/or cyclin D1. E) Clonogenic survival post UV (5 J/m^2) +/-siRNA against Dyrk1A and/or cyclin D1. (F) Effect of the ATR inhibitor VE-821 (10 µM) on removal of 6-4PP +/- siRNA against cyclin D1. Values are means +/- SD of at least 3 independent experiments (unpaired t test: ** $p < 0.01$; ***$p < 0.001$).

Figure 3: SPR defects caused by Dyrk1A depletion in Hela cells are not due to abnormal cell cycle progression or replicative stress-induced reduction in RPA availability

A) Left: chromatin-bound MCM7 detected by flow cytometry. S phase cells were gated using EdU incorporation signal. Each phase is represented by a different color. Right: fluorescence intensity of chromatin-bound MCM7 in early S phase (boxed in left panel) for siRNA against

Dyrk1A relative to NT controls. B) Chromatin-bound PCNA detected by flow cytometry. C) Cells were pretreated or not with Cdc7 inhibitor (1 µM PHA-767491) for 24 h. Left: cell cycle distribution quantified by EdU incorporation. Right: fluorescence intensity of EdU incorporation. D) Chromatin-bound PCNA as in B. E) Removal of 6-4PP 5 h post-UV after treatment with cdc7i. 10 µM. ATRi was used as control for defective SPR. F) Phosphorylation of Chk1 and RPA32 at 3h after 20 J/m^2 UV +/- siDyrk1A. G) Induction of γ-H2AX 1h +/- siDyrk1A after 20 J/m^2 UV was measured as a function of cell cycle by flow cytometry. H) Left: DNA-bound RPA32 was measured +/- siDyrk1A by flow cytometry 1h after 20 J/m^2 or 10 mM HU. Cells in S were labeled by EdU incorporation. The box delineates cells with high levels of chromatin-bound RPA. Right: quantification of S phase cells with elevated DNA-bound RPA from the left panel. I) Left: Immunoblot analysis of RPA subunits from whole cellular extracts treated with siRNA against Dyrk1A or siNT. Right: nuclear levels of total RPA measured by immunofluorescence. Nuclear intensities of total RPA32 or RPA70 were quantified from microscopy images. Mean intensities of RPA32 or RPA70 subunits in EdU+ cells were quantified for siRNA against Dyrk1A or NT controls. Values are means +/- SD of at least 3 independent experiments (unpaired t test: ** $p < 0.01$; ***$p < 0.001$).

Figure 4: Cyclin D1 overexpression causes an SPR defect in melanoma cell lines.

A) Immunoblot analysis of cyclin D1 expression from total protein extracts of 7 melanoma cell lines. B) Left: Immunoblot of cyclin D1 knock-down by siRNA in WM278 and 451Lu. Right: removal of 6-4PP 5 h after 20 J/m^2 UV. C) Stable expression of Flag-HA-cyclin D1 (WT or T286A) in WM1366 using a retroviral construct (Flag-HA-GFP is used as control). D) Immunoblot of Rb and phospho-Rb in WM1366 +/- cyclin D1(T286A), pretreated or not for 4 h

with 10 µM palbociclib. E) Cell cycle distribution +/- palbociclib (24 h treatment). F) Effect of cyclin D1(T286A) overexpression on 6-4PP removal. Cells were pretreated (or not) with palbociclib for 4 h, and the drug was maintained in the medium during post-UV incubation. G) UV sensitivity measured by clonogenic survival. H) Induction of DSB in WM1366 detected by phospho-53BP1(S1778) and γH2AX co-labeling 16 h after 20 J/m^2 UV. I) Apoptosis assessed by caspase 3 and PARP1 cleavage 16h after UV (1 µM staurosporine for 3 h as control). For all panels in this figure, error bars represent the average +/- SD of at least 3 independent experiments (unpaired t test: ** $p < 0.01$; ***$p < 0.001$).

Figure 5: Increased p21 levels are responsible for SPR defects caused by abnormal stabilization of cyclin D1 in melanoma cells.

A) Immunoblot of p21 from total protein extracts +/- cyclin D1 (T286A). B) Nuclear levels of HA-tagged cyclin D1 in EdU(-) and EdU(+) cells measured by immunofluorescence. C) Nuclear levels of p21 measured by Immunofluorescence. D) Left: Immunoblot of p21 and cyclin D1 +/- siP21. Middle: cell-cycle distribution +/- siP21. Right: removal of 6-4PP +/- siP21. E) Unscheduled DNA synthesis (UDS) in Hela cells treated with siRNA against Dyrk1A or XPA (NER deficient control). Left: Immunoblots showing knock-down of Dyrl1A and XPA. Right: Quantification of UDS via EdU incorporation in G1/G2 2 h after treatment or mock-treatment with 20 J/m^2 UV. Error bars represent the average +/- SD of at least 3 independent experiments (unpaired t test: ** $p < 0.01$; ***$p < 0.001$).

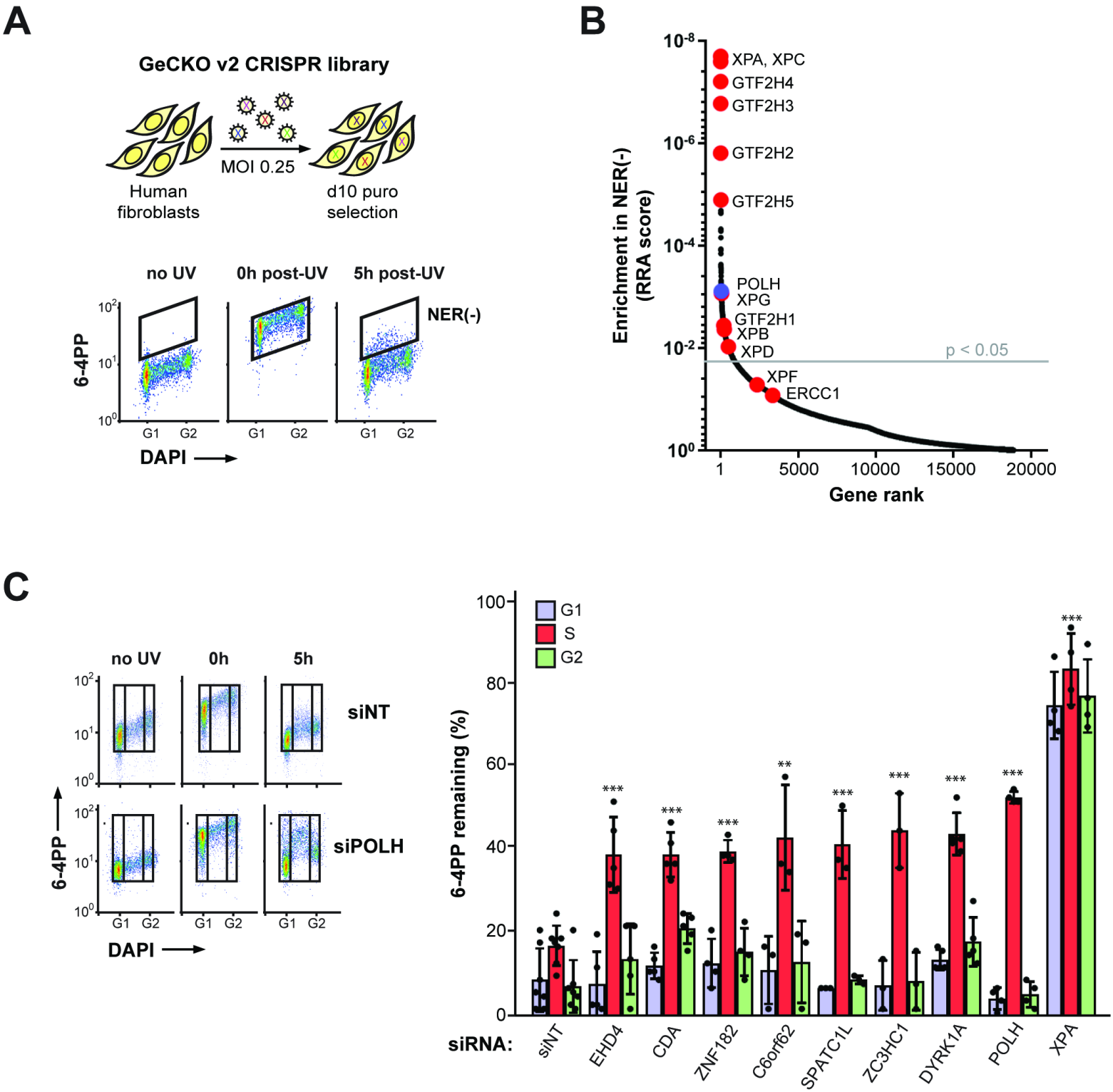
A
GeCKO v2 CRISPR library
MOI 0.25
Human fibroblasts
d10 puro selection
no UV
0h post-UV
5h post-UV
NER(-)
6-4PP
DAPI
G1
G2
B
Enrichment in NER(-) (RRA score)
Gene rank
XPA, XPC
GTF2H4
GTF2H3
GTF2H2
GTF2H5
POLH
XPG
GTF2H1
XPB
XPD
XPF
ERCC1
p < 0.05
C
no UV
0h
5h
siNT
siPOLH
6-4PP remaining (%)
G1
S
G2
siRNA:
siNT
EHD4
CDA
ZNF182
C6orf62
SPATC1L
ZC3HC1
DYRK1A
POLH
XPA

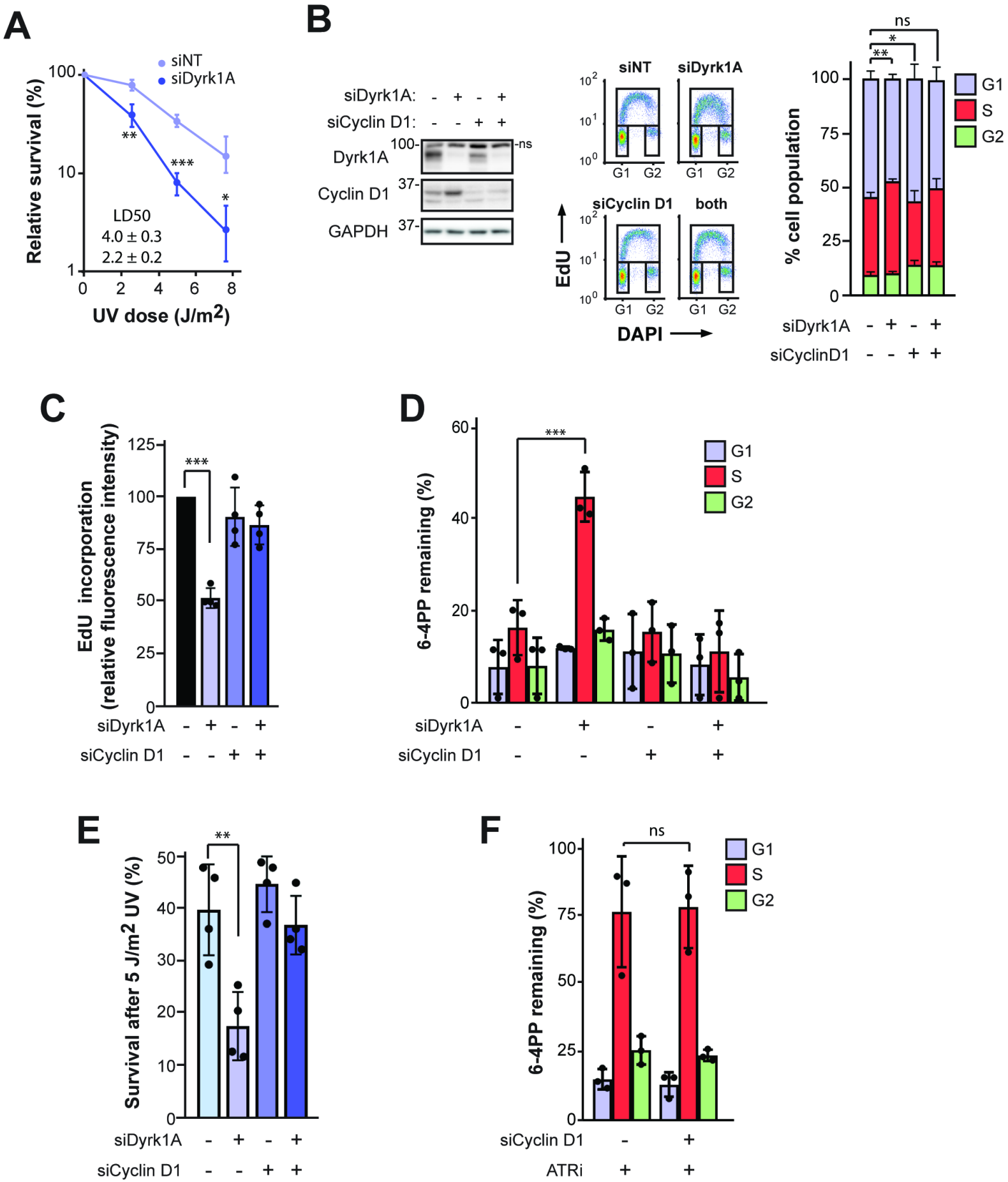
A
siNT
siDyrk1A
Relative survival (%)
100
10
1
**
***
*
LD50
4.0 ± 0.3
2.2 ± 0.2
0
2
4
6
8
UV dose (J/m2)
B
siDyrk1A: - + - +
siCyclin D1: - - + +
Dyrk1A
Cyclin D1
GAPDH
100-
37-
37-
-ns
siNT
siDyrk1A
siCyclin D1
both
EdU
DAPI
G1
G2
ns
*
**
% cell population
G1
S
G2
siDyrk1A - + - +
siCyclinD1 - - + +
C
EdU incorporation
(relative fluorescence intensity)
125
100
75
50
25
0
***
siDyrk1A - + - +
siCyclin D1 - - + +
D
6-4PP remaining (%)
60
40
20
0
***
G1
S
G2
siDyrk1A - + - +
siCyclin D1 - - + +
E
Survival after 5 J/m2 UV (%)
50
40
30
20
10
0
**
siDyrk1A - + - +
siCyclin D1 - - + +
F
6-4PP remaining (%)
100
75
50
25
0
ns
G1
S
G2
siCyclin D1 - +
ATRi + +

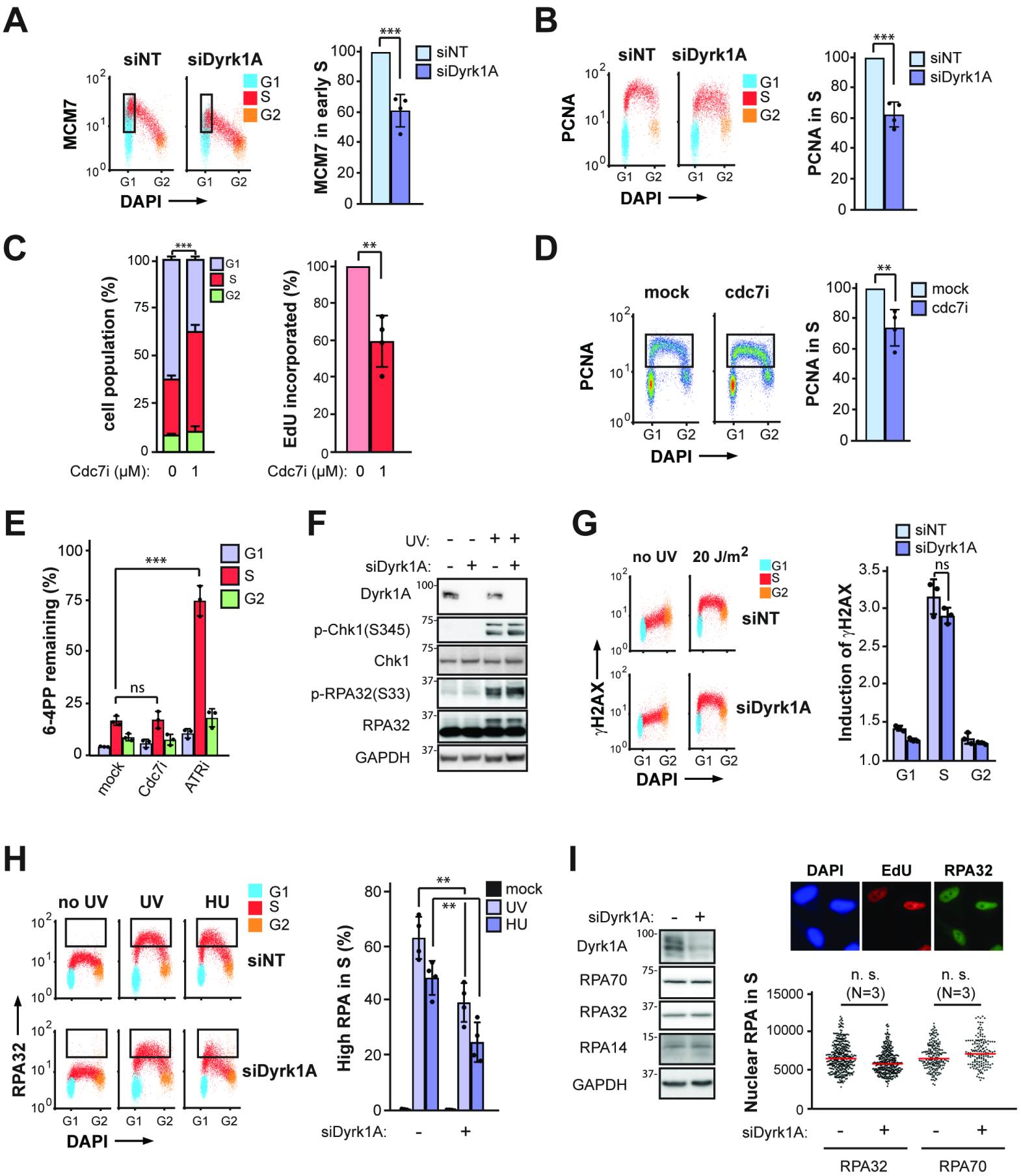
A
siNT
siDyrk1A
MCM7
DAPI
G1
S
G2
MCM7 in early S
siNT
siDyrk1A
***
B
PCNA in S
C
cell population (%)
EdU incorporated (%)
Cdc7i (μM): 0 1
**
D
mock
cdc7i
E
6-4PP remaining (%)
ns
ATRi
F
UV:
siDyrk1A:
Dyrk1A
p-Chk1(S345)
Chk1
p-RPA32(S33)
RPA32
GAPDH
G
no UV
20 J/m2
γH2AX
Induction of γH2AX
H
HU
RPA32
High RPA in S (%)
mock
UV
I
Nuclear RPA in S
n. s.
(N=3)
RPA70

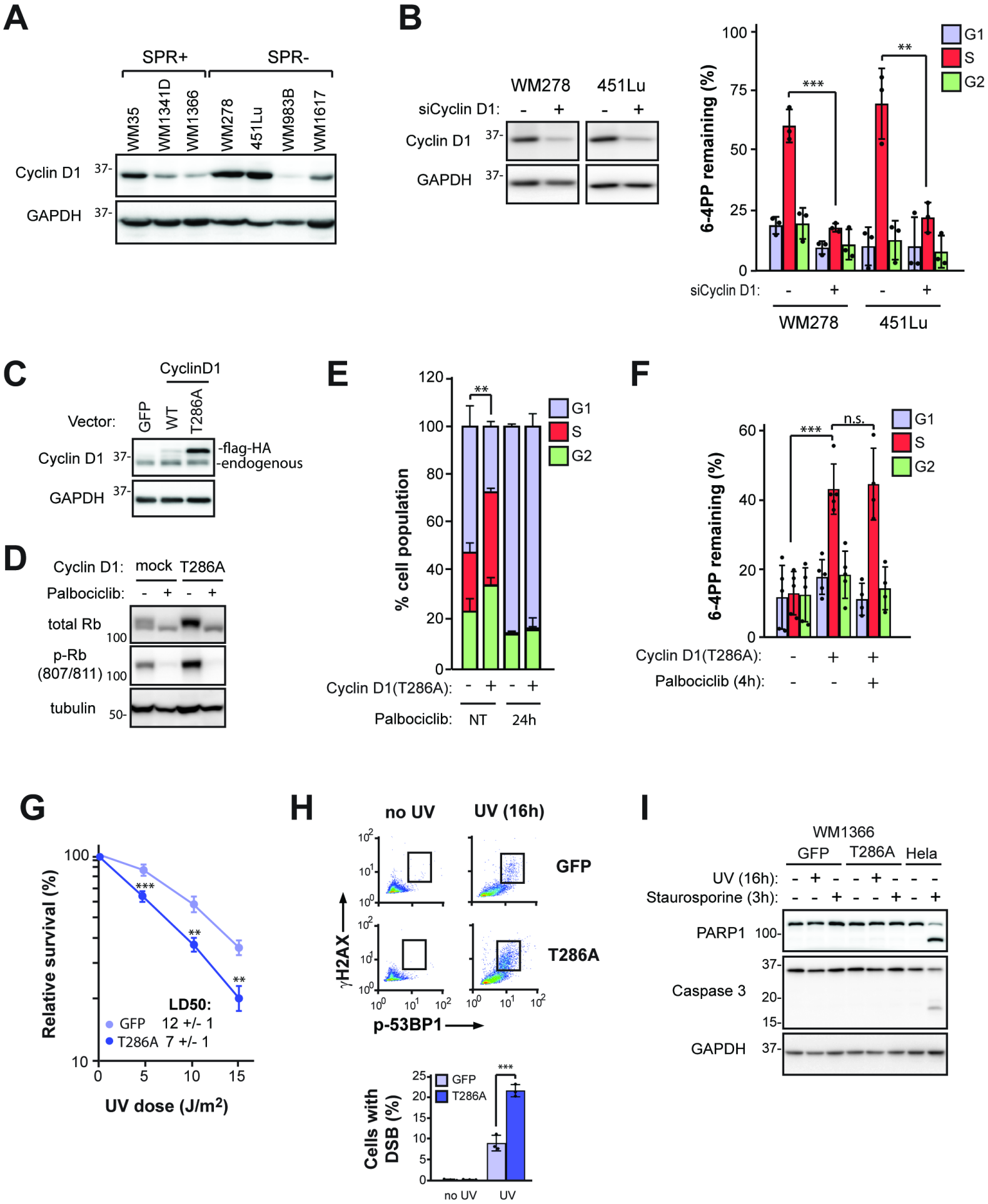
A
SPR+
SPR-
WM35
WM1341D
WM1366
WM278
451Lu
WM983B
WM1617
Cyclin D1
GAPDH
37-
B
WM278
451Lu
siCyclin D1:
Cyclin D1
GAPDH
6-4PP remaining (%)
G1
S
G2
***
**
siCyclin D1:
WM278
451Lu
C
CyclinD1
Vector:
GFP
WT
T286A
Cyclin D1
-flag-HA
-endogenous
GAPDH
D
Cyclin D1:
mock
T286A
Palbociclib:
total Rb
p-Rb (807/811)
tubulin
100
50-
E
% cell population
Cyclin D1(T286A):
Palbociclib:
NT
24h
F
6-4PP remaining (%)
n.s.
Cyclin D1(T286A):
Palbociclib (4h):
G
Relative survival (%)
UV dose (J/m2)
LD50:
GFP 12 +/- 1
T286A 7 +/- 1
H
no UV
UV (16h)
GFP
T286A
γH2AX
p-53BP1
Cells with DSB (%)
no UV
UV
I
WM1366
GFP
T286A
Hela
UV (16h):
Staurosporine (3h):
PARP1
Caspase 3
GAPDH

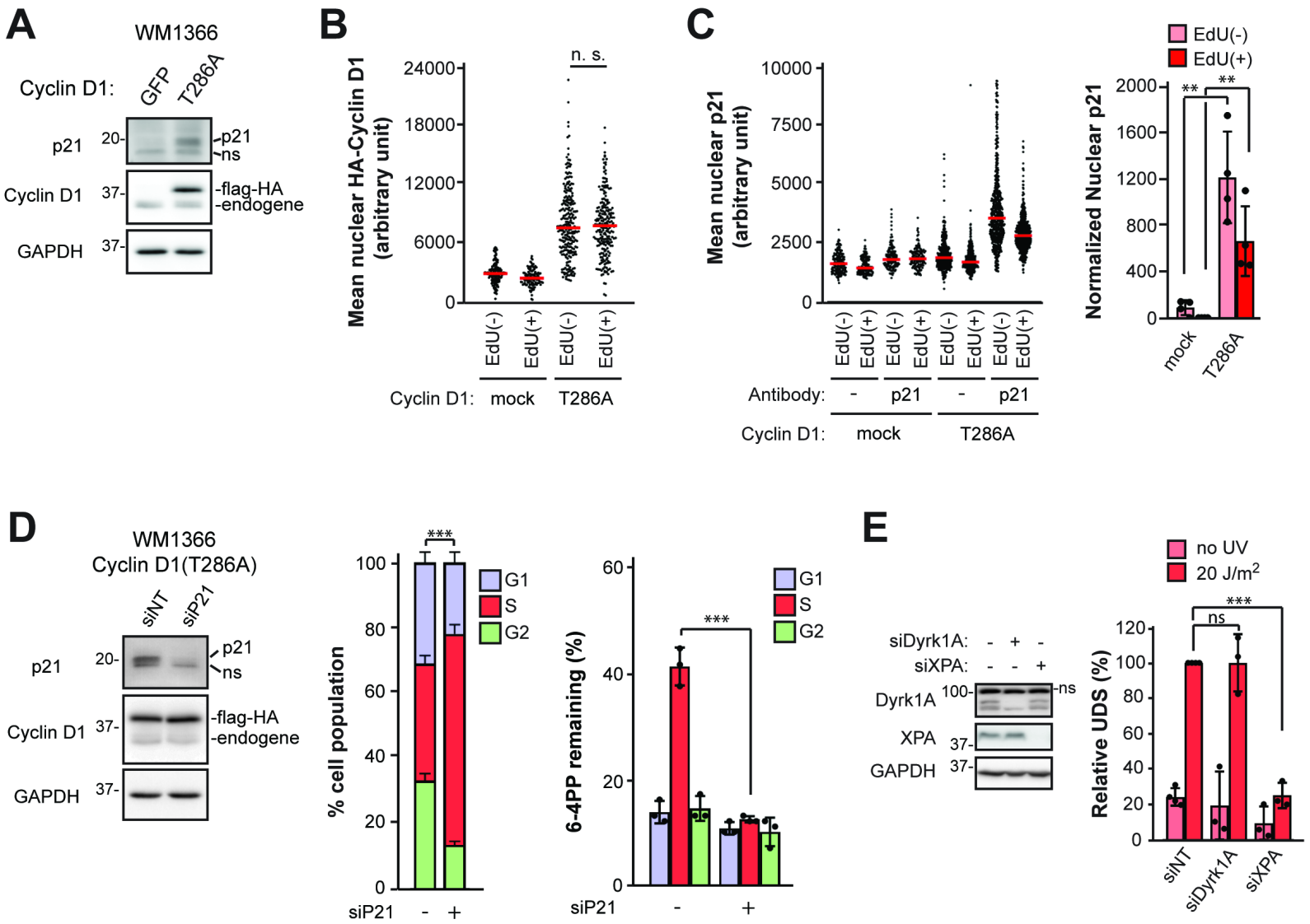
A
WM1366
Cyclin D1:
GFP
T286A
p21
20-
p21
ns
Cyclin D1
37-
-flag-HA
-endogene
GAPDH
37-
B
Mean nuclear HA-Cyclin D1 (arbitrary unit)
24000
18000
12000
6000
0
n. s.
EdU(-)
EdU(+)
EdU(-)
EdU(+)
Cyclin D1:
mock
T286A
C
Mean nuclear p21 (arbitrary unit)
10000
7500
5000
2500
0
EdU(-)
EdU(+)
EdU(-)
EdU(+)
EdU(-)
EdU(+)
EdU(-)
EdU(+)
Antibody:
-
p21
-
p21
Cyclin D1:
mock
T286A
EdU(-)
EdU(+)
Normalized Nuclear p21
2000
1600
1200
800
400
0
**
**
mock
T286A
D
WM1366
Cyclin D1(T286A)
siNT
siP21
p21
20-
p21
ns
Cyclin D1
37-
-flag-HA
-endogene
GAPDH
37-
% cell population
100
80
60
40
20
0
***
G1
S
G2
siP21
-
+
6-4PP remaining (%)
60
40
20
0
***
G1
S
G2
siP21
-
+
E
siDyrk1A:
-
+
-
siXPA:
-
-
+
Dyrk1A
100-
-ns
XPA
37-
GAPDH
37-
no UV
20 J/m2
Relative UDS (%)
120
100
80
60
40
20
0
***
ns
siNT
siDyrk1A
siXPA